Studies on Partially Melted Zone and Pitting Corrosion Resistance of A356 Aluminium–Silicon Alloy GTA Welds

K. Ratna Kumar[1] G. Madhusudhan Reddy[2] and K. Srinivasa Rao[3]
[1]Department of Metallurgical Engineering, Government Polytechnic, Visakhapatnam- 530 007
[2]Metal Joining Group, Defence Metallurgical Research Laboratory, Hyderabad-500 058
[3]Department of Metallurgical Engineering, Andhra University College of Engineering(A), Visakhapatnam- 530 003

ABSTRACT

Gas Tungsten Arc Welding (GTAW) of Pressure Die cast A356 Al-Si alloy with strontium modification was done both with and without filler. The microstructural changes in Weld metal zone (WM), Heat affected zone (HAZ) and Partially Melted Zone (PMZ) were studied. PMZ of aluminium alloy weld is an important region, as it is the weak link in the weldments. It is significantly affected by the welding parameters, filler metal and prior thermal condition. In the present work affect of welding techniques i.e. Continuous Current Gas Tungsten Arc Welding (CCGTAW) and pulsed Current Gas Tungsten Arc Welding (PCGTAW) on microstructure and pitting corrosion resistance of weld metal, Partially melted zone and Heat affected zone in the prior conditions   of as cast and T6 conditions were studied. Susceptibility to liquation was found to be less in the weld made in as cast condition of pulsed current GTA welds compared to that of artificially aged condition (T6) of continuous current GTA welds. This was mainly attributed to the silicon enrichment of eutectics at the grain boundaries. Potentiodynamic polarization testing was carried out to study the pitting corrosion behavior of the welds. Pitting corrosion resistance of weld made with pulsed current GTAW of as cast alloy is better than the that of weld made with continuous current GTAW of T6 alloy. This is mainly attributed to the discontinuous eutectic formation at the grain boundary base metal and PMZ.

Key words: Aluminium alloys, GTA Welds, Partially Melted Zone, Continuous Current gas tungsten arc welding, Pulsed current gas tungsten arc welding.
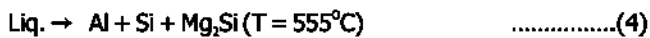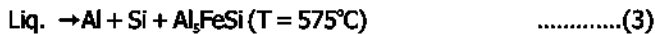
1.0   INTRODUCTION

Cast aluminium alloys are most widely used for automotive industries. The mechanical properties of cast aluminum alloys are largely dependent upon the solidification microstructure of the alloys [1, 2]. Many authors have studied the microstructure of A356 and the effects of additives on the mechanical behavior of the alloy. Liu and Kim observed α-Al plus several morphologically distinct intermetallic constituents as well as Si phase in the α-Al inter dendritic regions of the cast alloy [3, 4]. The β (AlB$_5$BFeSi) phase generally appeared with platelet morphology [4]. The intermetallic compound π

(AlB$_8$BSiB$_6$BMgB$_3$BFe) appeared as typical lamellar or "Chinese-script" structure [4, 5]. MgB$_2$BSI phase, with a Chinese script structure, was also observed in the inter- dendritic regions [4, 6]. These intermetallic phases were all the products of eutectic reactions [7]. Following reactions occur in the system as the alloy is cooled, although the formation of each intermetallic depends on cooling rate and amounts of each constituting elements [4, 5].

Development of Dendritic network (T = 614°C) ....(1)

Liq. $\rightarrow$ Al + Al$_{15}$(Mn,Fe)$_3$Si$_2$(T = 594°C)   .... (2a)

27

$$Liq. \rightarrow Al + Al_5FeSi + Al5FeSi + Al_{15}(Mn,Fe)_3Si_2 (T = 594°C) ... (2b)$$

$$Liq. \rightarrow Al + Si + Al_5FeSi (T = 575°C) \qquad ....(3)$$

$$Liq. \rightarrow Al + Si + Mg_2Si (T = 555°C) \qquad ....(4)$$

$$Liq. \rightarrow Al + Si + Mg_2Si + Al_8Si_6Mg_3Fe (T = 554°C) \qquad ....(5)$$

The partially melted zone (PMZ) is a region immediately outside the weld metal where liquation can occur during welding and lead to hot cracking and degradation of mechanical properties [8]. Intermetallic phases present in the alloys induce liquation in the PMZ by the eutectic reaction with surrounding matrix. Formation of type of inter metallics in Al-alloys mainly is controlled by the alloying elements and thermal temper. However, besides Mg and Si also other elements such as Fe (0.8%) and Mn (0.8%) can be present. Since Fe has a very low solubility in the Al-matrix, almost all Fe present in the alloy will bind with the excess of Si and the abundant Al to form typically one volume percent of Fe-containing inter metallics [9]. During solidification, these inter metallics form at the edges of the aluminum dendrites by an eutectic reaction, which explains their plate like shape.

Huang and Kou recently studied PMZ liquation in the Gas metal arc welds of alloys AA2219, AA2024, AA6061 and AA7075, including the liquation mechanisms and found that significant weakening of the PMZ is caused by GB segregation [10-13]. Even though the preferred welding method for aluminium alloys is alternating current GTA welding process, several investigators have identified a number of advantages of the pulsed current technique including increased control of microstructure, reduced grain size, refined solidification structure and reduced segregation of alloying elements [14-17]. Madhusudhan Reddy in his studies proved that pulsed current application improved the weldability, strength and corrosion properties of aluminium-lithium alloy welds [18]. Liquation and liquation-induced hot cracking in aluminium alloys AA2024, AA6061 and AA7075 have been studied and attention appeared to have been focused much more on the liquation-induced hot cracking than liquation itself [19-29].

The resistance to corrosion of aluminium alloy welds is affected by the alloy being used, the filler alloy and the welding process used. When localized corrosion does occur in aluminium welds, it may take the form of preferential attack of the weld bead, pitting, intergranular attack of exfoliation may occur in the heat affected zone (HAZ). Welds in Al-Mg-Si alloys (AA6061) generally have good resistance to atmospheric corrosion, but

in specifically corrosion environments like sea water, localized corrosion may occur. Some heat treatable alloys particularly those containing substantial amounts of copper and zinc, may have their resistance to corrosion lowered by the heat of weld. These alloys exhibit grain boundary precipitation in the HAZ and this zone can be anodic to the remainder of the weldment. Welds in the Al-Zn-Mg alloys were seen to be attacked preferentially in the area adjacent to the weld bead when exposed to a corrosive environment in the as weld condition [30]. Galvanic cells that cause corrosion can be created because of the corrosion potential differences among the base metal, the filler metal and heat affected regions where microstructural changes have been produced. In some alloys intermetallic phases formed by the base metal determine the final corrosion resistance of the weld, for example Mg_2Si in AA6061 Al alloys are harmful with respect to weldability and corrosion resistance. These intermetalic particles induce liquation in partially melted zone (PMZ) of the weldment, leading to cracking and galvanic coupling of these phases with the surrounding matrix resulting in poor corrosion resistance. Conventional continuous current welding (CCW) techniques of gas tungsten arc welding (CCTIG) significantly affect properties such as strength and corrosion resistance[31].

Detailed studies on the effect of prior thermal temper and welding technique on the PMZ behavior and pitting corrosion behaviour of cast aluminium alloys are not available in the literature. In the present study A356 Al-Si alloy is selected because it is widely used for automotive applications and liquation susceptible during welding. The present investigation aims at finding out variation in the microstructure and hardness of Continuous Current Gas Tungsten Arc (CCGTA) welds and Pulsed Current Gas Tungsten Arc (PCGTA) welds of A356 alloy both by using 5356 filler and without filler in the initial thermal tempers of T-6 and as cast condition. The variations in pitting corrosion behavior in above conditions are also investigated.

2.0 EXPERIMENTAL DETAILS

Low pressure Die cast A356 Al-Si alloy plates of thickness 10mm in as cast and T-6 (Solution treatment at 530°C-1 hour and aged at 140°C-8 hours) are being used. Chemical composition of the base metal is given in the **Table 1**. Gas-Tungsten Arc bead-on plate Welds were made. The common welding parameters in Continuous current GTA welding and pulsed current GTA welding are given in **Table 2** and **Table 3** respectively. The above procedure was repeated by using 5356

filler material. The samples of base metal and welds with PMZ were polished on emery papers and disc cloth to remove the very fine scratches. Polished surfaces are etched with HF reagent. Optical microscopy (OM) has been done on the both top surface and transverse section of the weld. The locations where the microstructures of PMZ taken are shown in **Fig. 1.** The microstructures were recorded with Image analyzer attached to the Metallurgical microscope and are given in the **Figs.3-10**. Vickers hardness testing has been carried out on Weld, PMZ and Heat affected zone areas of the samples with 5 kgf load. The hardness profiles are prepared cross the weldment and are reported in **Fig. 11** and **Fig.12**. A software based PAR Basic electrochemical system was used to make potentiodynamic polarization tests to study the pitting corrosion behaviour of the base metal, HAZ and PMZ regions. A saturated calomel electrode (SCE) and carbon electrode were used as reference and auxiliary electrodes respectively. All experiments were conducted in aerated 3.5% NaCl solutions with pH adjusted to 10 by adding potassium hydroxide. The potential scan was carried out at 0.166 mVs^{-1} with the initial potential of –0.25 V (OC) SCE to the final pitting potential. The exposure area for these experiments was 1 cm^2. The potential at which current increased drastically was considered to be the critical pitting corrosion E$_{pit}$. Specimens exhibiting relatively more passive potential (or less negative potentials) were considered to have better pitting corrosion resistance. Optical microscopy on dynamically polarized samples was carried out to understand the mechanism of pitting. The critical dynamically polarized curves are given in the **Figs.13-16.** The microstructures on corroded regions i.e WM, PMA avd HAZ were recorded with Image analyzer attached to the Metallurgical microscope and are given in the **Fig-17.**

3.0 RESULTS AND DISCUSSION

3.1 Base Metal studies

Average composition of the base metal is given in **Table 1.**The available silicon for forming Mg$_2$Si is calculated as [32]

Available Silicon = % Si – ¼ (%Fe + %Mn)

Table 1 also gives the amount of inclusions and dispersiod present in the alloy estimated from the composition. It is assumed that all the available iron forms into inclusions. Optical micrographs of the base metals are shown in the **Fig. 3**. The grain structure is well developed. Coarse particles of Si-rich eutectics (dark) and Fe$_3$SiAl$_{12}$ (grey) are clustered in stringers and aligned. Micrographs reveal that more number of
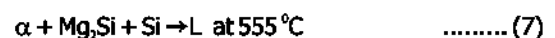
Si-rich particles are present in artificially aged (T6) alloy when compared to that of as cast alloy.

3.2 Liquation in Partially melted Zone of GTA Welds

Heat affected zone was observed near the fusion line as shown in the micrographs (**Figs.6, 7** and **8**). It can be observed that coarsened grain boundaries occurred adjacent to the fusion line. Coarsening of grain boundaries indicated partial melting of A356 alloy GTA welds. Optical micrographs of A356-T6 GTA-weld show clearly the dark etched grain boundaries indicating the liquation in the PMZ. Grain boundary filled with eutectic liquid can be seen in the optical micrographs. In general aluminium liquids that are richer in silicon are considered to be more fluid and penetration should be easier for the A356 alloy and lower solidus temperature of the alloy might have promoted liquid penetration to the HAZ for a longer distance [33].

Recently Huang C and Kou [11] proposed three different liquation mechanisms in the partial melted zone of wrought multi-component aluminum alloys during welding. For alloys behind the solid solubility limit, liquation-induced particles react with a matrix and liquation can occur at any heating rate (Mechanism I). For alloys within the limit but with liquation-induced particles, liquation requires high heating rate (Mechanism II). For alloys within the limit and without such particles, liquation occurs when the aluminum starts to melt (Mechanism III). Liquation causing particles in the alloy 6061 are proposed in their study are not Mg$_2$ Si but Silicon rich particles with varying Mg, Cu and Zn contents. Fe-rich particles do not appear to cause liquation. The eutectic particles identified in the PMZ are not Al- Mg2Si eutectic particles, but eutectic particles consisting of Si-rich and Fe-rich phases. Severe grain boundary segregation of Si and Mg is noticed in the case of GMA Welds of 6061 alloys.

Hence the possible eutectic reactions [34] causing liquation in PMZ of the welds of the present investigation are as follows.

$$\alpha + Si \rightarrow L \quad \text{at} \quad 577^{\circ}C \quad \text{.........(6)}$$

$$\alpha + Mg_2Si + Si \rightarrow L \text{ at } 555^{\circ}C \quad \text{.........(7)}$$

Optical microscopy indicated the silicon enrichment of the particles at the areas prone to liquation.

3.3 Effect of prior condition

In the present work Optical observation (**Figs. 6** and **7**) of the PMZ areas of the welds shows that grain boundary melting and coarsening of PMZ is severe in T-6 condition compared to that

of as cast condition. Coarser grain size in HAZ in T6-condition, when compared to that of as cast condition may be due to higher concentration of Silicon and magnesium at the grain boundaries. Higher concentration of Mg and Si at grain boundaries could lower the solidus temperature locally and make the grain boundaries more susceptible to liquation during welding. It is evident that Silicon rich eutectic is more at the GBs of PMZ in the welds of T6 compared to that of as cast condition.

3.4 Effect of prior welding technique

Hardness curves of A356 GTA welds have been shown in **Figs. 11** and **12**. It is very clear that PMZ hardness is more in CC welds than that of PC welds. Optical photographs (**Figs.9** and **10**) show that eutectic concentration at the GBs is relatively less for PC welds compared to that of CC welds. Grain coarsening has been found to be less in the PC welds. Similar trend has been observed in the A356 as cast welds and it is attributed to the following effects caused by the Pulsed current GTA welding.

Pulsed GTA welding is a variation of GTA welding which involves cycling of the welding current from a high level to a low level at a selected regular frequency. The high level or the peak rent is generally selected to give adequate penetration and bead contour, while the low level or the background current is set at level sufficient to maintain a stable arc. This permits arc energy to be used efficiently to fuse a spot of controlled dimensions in a short time producing the weld as a series of overlapping nuggets and limits the wastage of heat by conduction into the adjacent parent material in normal constant current welding. In contrast to constant current welding, the fact that heat energy required to melt the base material is supplied only during peak current pulses for brief intervals of time allows the heat to dissipate into the base material during the back ground current time and thus lowers heat build up in the adjacent base material leading to a narrower heat-affected zone (HAZ). Metallurgical advantages of pulsed current (PC) welding frequently reported in literature include refinement of fusion zone grain size and substructure, reduced width of HAZ, control of segregation, etc (**Figs. 8** and **9**). All these factors help in improving weld mechanical properties.

Kou S and Le Y proved that structure and properties of aluminum welds are improved significantly by low frequency oscillation GTAW. The extent of grain boundary melting is less severe with arc oscillation and less severity of PMZ has been attributed to the higher resultant velocity of the weld pool during oscillated arc welding that decreases the distance between isotherms T_L (liquidus) and T_E (Eutectic). Hence the extent of grain boundary melting in PMZ was reduced by arc oscillation [35].

The periodic variations in the arc current in Pulsed current GTAW will also result in similar changes in the arc forces impinging on the weld puddle, which are proportional to the square of the welding current. These variations in the arc forces enhance convective forces already existing in the weld pool. The enhanced fluid motion in the weld pool homogenizes the weld metal composition and helps in reducing the segregation and porosity. Another consequence of the enhanced weld pool turbulence is a reduction in temperature gradients and peak temperatures in the weld pool and the HAZ.

3.5 Effect of filler metal

Optical micrographs of fusion zone of A356 GTA welds made with and without filler AA5356 are as shown in **Figs.4** and **5**. Fusion zone of Autogeneous weld contained relatively more continuous interdendritic eutectic and was identified as Al-Si eutectic. In addition to dendritic network, relatively coarser grains were observed in the fusion zone of Autogeneous weld. Fusion zone microstructure of AA5356 filler was found to contain predominantly discontinuous interdendritic network, which was generally identified as Al-Mg2Al3 eutectic [36]. Globules of dendrites were seen predominantly in the fusion zone made by pulsed current GTAW. Optical micrographs of PMZ (**Fig. 6** and **7**) reveal that width of the PMZ in weld made with 5356 filler is less than that of autogeneous weld. This may be attributed to the possible reduction in the interdendritic diffusion of Silicon due to the presence of Al-Mg$_2$Al$_3$ eutectic. Further refinement of dendrites in PMZ of weld made with 5356 filler is also evident from the optical micrographs (**Fig. 7**).

3.6 Hardness Testing

Observed higher hardness in PMZ of both the alloys of GTA weld (**Fig.11** and **12**) may be attributed to the silicon rich eutectic formed by the reaction of the Mechanism II proposed by Huang and Kou [13]. In autogeneous welds, hardness of PMZ is higher in T6 condition compared to as cast condition. Reverse trend is observed with the use of Filler. This may be attributed to the presence of Mg$_2$Si precipitates in T6 condition of the alloy. Therefore multi component, A356 Al- alloy are highly prone to liquation in PMZ when welded in artificially aged T6 condition compared to welds in as cast condition. This can be reduced by the use of Filler

3.7 Pitting corrosion of BM, PMZ and HAZ of GTA welds

The potential at which current increased drastically was considered as the critical pitting potential and the values are given in **Table 4 - 6**. The influence of prior condition is seen clearly on the pitting corrosion resistance of the base metal and HAZ which also included the PMZ. The typical potentiodynamic curves for base metal and welds are given in **Figs. 13-16**. The pitting corrosion resistance of the PMZ was poor in artificially aged (T6) condition of the alloy when compare with as cast condition. The weld metal zone and PMZ of pulsed current GTA welded as cast alloy shows better corrosion resistance than Continuous current GTA welded T6 alloy. The typical optical micrographs of the dynamically polarized WM and PMZs of A356 GTA welds are shown in **Figs. 17**. It is very interesting to note that the pitting was severe around the PMZ area of the A356 GTA welds both in continuous and pulsed current mode. This was attributed to the precipitation of intermetallics in the PMZ area. Severe pitting was observed at the grain boundaries in the PMZ and base metal. This was attributed to the discontinuous eutectic formation at the grain boundary in both base metal and PMZ.

4.0 CONCLUSIONS

1. Eutectic reaction of excess silicon rich particles with surrounding α- matrix and back filling of silicon rich liquid from the weld pool causes liquation in GTA welds of Alloy A356.

2. Grain coarsening and melting in PMZ is more when the Alloy A356 is welded in T-6 temper than in as cast condition.

3. Pulsed current GTAW has reduced the liquation in partially melted zone of Alloy A356 welds compared to that of Continuous current GTAW.

4. Prior thermal temper and the welding technique play important role in the liquation of partially melted zone of the heat treatable Aluminium alloy Welds.

5. Width of the PMZ is less with the use of AA5356 Filler compared to autogeneous weld.

6. Pitting corrosion resistance of the weld metal zone and PMZ of the PCGTA welded as cast alloy is more than that of the CCGTA welded T6 alloy.

7. Pitting corrosion resistance of the weld metal zone and PMZ of the autogenuous GTA weld is more than that of the 5356 filler welds.

REFERENCES

[1]. J. A. J. Griffin and F. R. Brotzen, Journal of the Electrochemical Society, 1994.141(12): p. 3473-3479.

[2]. A. K. Bhattamishra and K. Lal, Effect of Si and Cr on the Intergranular Corrosion in Al-Si-Mg Alloys. Materials and Design, 1997.18 (1)

[3]. A. M. Samuel and F. H. Samuel, Journal of Materials Science, 1995. 30(7): p. 1698-1708.

[4]. A. M. M. M. Adam, N. Borras, E. Perez and P. L. Cabot, Journal of Power Sources, 1996. 58: p. 197-203.

[5]. S. S. A. E. Rehim, H. H. Hassan and M. A. Amin, Corrosion Science, 2003. 46 (2004)(1): p. 5-25.

[6]. Aluminum Casting Technology I. American Foundrymen's Society. 2nd ed.c1986: Des Plaines, Ill, American Foundrymen's Society. 359.

[7]. F. Andreatta, H. Terryn and J. H. W. d. Wit, Effect of Solution Heat Treatment on Galvanic Coupling between Intermetallics and Matrix in Aa7075-T6. Corrosion Science, 2003. 45(8): p. 1733-1746.

[8]. Sindo Kou, Welding Metallurgy, second ed, John Wiley & Sons, USA, 2003.

[9]. C. M. Allen, K. A. Q. O'Reilly, B. Cantorand P. V. Evans: Progress in Material Science,1998,43, 89-170. [10].C.Huang, S.Kou., Welding Journal. 79 (2000) 113s-120s.

[11]. C.Huang, S.Kou., Welding Journal. 81 (2002) 211s-222s.

[12]. C. Huang, S. Kou., Welding Journal. 80 (2001) 46s-53s.

[13]. C. Huang, S. Kou. Welding Journal. 80 (2001) 9s-17s.

[14]. J. G. Garland, Met.const.Br.Weld.J. 6 (1974)121-127.

[15]. G. M. Reddy, J. Mater. Sci. 32(1997) 4117-4124.

[16]. H. Yamamoto, Weld. Int. 7(1993) 456-467.

[17]. G. D. Janaki Ram, Practical Metallography. 37 (2000) 276-284.

[18]. G. Madhusudana Reddy, Ph.D Thesis, IIT-Madras,(1998) 323-328

[19]. J. B. Arthur: Welding Journal., 1955, 34,558s-569s.

[20]. F. R. Collins: Welding Journal., 1962, 41,337s-345s.

[21]. D. E. Schillinger, I. G. Betz, F. W. Hussey and H. Markus: Welding Journal.,1963,42,269s- 275s.

[22]. R. E. Fish and C. S. Shira: Welding Journal., 1966, 45,490s-496s.

[23]. J. H. Dudas and F. R. Collins: Welding Journal., 1966, 45,241s-249s.

[24]. G. E. Metzger: Welding Journal., 1967, 457s-469s.

[25]. J. E. Steenbergen and H. R. Thorton: Welding Journal.,1970,49,61s-68s.

[26]. N. F. Gittos and M. H. Scott: Welding Journal., 1981,60,95s-103s.

[27]. M. Katoh and H. W. Kerr: Welding Journal., 1987, 66,360s-368s.

[28]. H. W. Kerr and M. Katoh: Welding Journal., 1987,66, 251s-259s.

[29]. M. Miyazaki, K. Nishio, M. Katoh, S. Mukae and H. W. Kerr: Welding Journal., 1990,69,362s- 371s.

[30]. L. F. Mondolfo: 'Aluminium alloy; Structure and properties', 1976, Butterworths & Co

[31]. J. R. Davis: 'Corrosion of aluminium alloy', 2nd edn; 2000,Ohie, ASM International.

[32]. R. C. Darward: Metall. Trans., 1973,4,508

[33]. M. Katoh and H. W. Kerr: Welding Journal.,1987, 66,360s-368s.

[34]. L. F. Mondolfo: 'Aluminium alloys: Structure and properties', 1976, Butterworths & Co

[35]. S.Kou and Y.Le: Welding Journal., 1985,64,51-55.

[36]. Metals Handbook 9th edition Vol.4, Heat treating, 678-679, 1981. Materials park, O.H., ASM International.

Table 1: Composition and constituents of the base metal A356

Element	Weight(%)
Mg	0.25-0.45
Si	6.5-7.5
Fe	01.2
Mn	0.10
Ni	0.05
Sr	0.05
Ti	0.05
Available Si	6.92

Table 2 : Welding parameters in Continuous current GTA Welding of A356 alloy

Parameter	Value
Voltage (V)	10-12
Current (Amp)	225
Welding speed (mm/min)	150
Gas flow rate (cft)	28

Table 3 : Welding parameters in pulsed current GTA Welding of A356 alloy

Parameter	Value
Ip/Ib	300/150
tp/tb	50%
Frequency (Hz)	6
Welding speed	150

Table 4 : E_{pit} values of the Base metal A356 alloy

Condition	E_{pit} Value (mV)
As cast	-716.0
T6	-684.7

Table 5 : E_{pit} values of the weld metal of GTA welded A356 alloy

Condition	Autogenous	5356 filler
AC-CC	-723.4	-697.7
AC-PC	-655.0	-669.6
T6-CC	-722.2	-706.8
T6-PC	-680.0	-684.3

Table 6 : E_{pit} values of the Partially Melted Zone of GTA welded A356 alloy

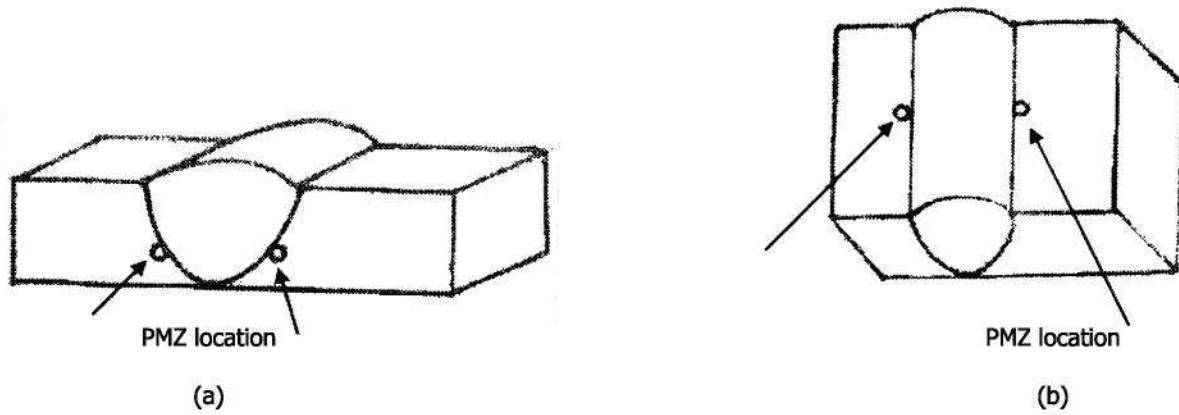| Condition	Autogenous	5356 filler
AC-CC	-705.8	-693.1
AC-PC	-669.1	-679.7
T6-CC	-722.7	-710.3
T6-PC	-698.0	-705.2

Fig. 1: Location of the PMZ where the photomicrographs are taken
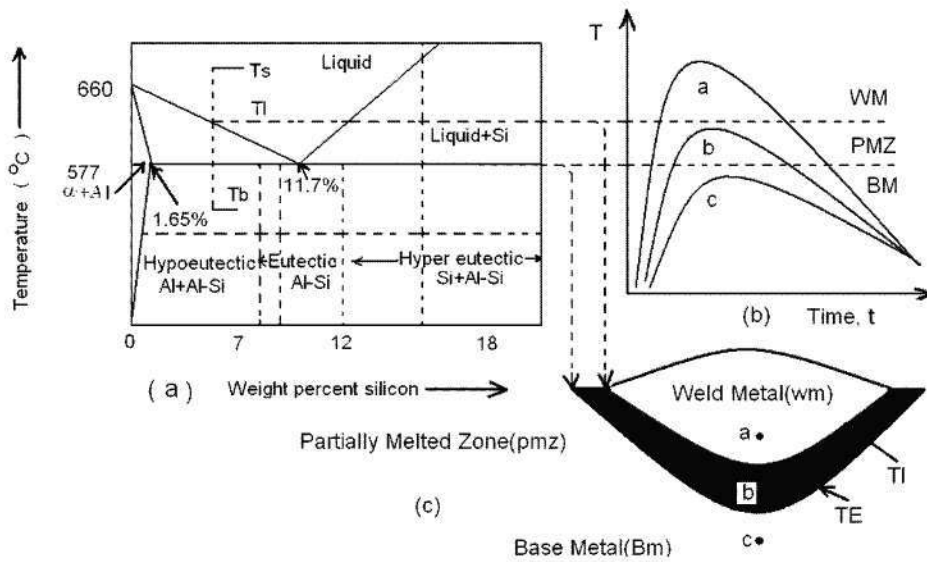
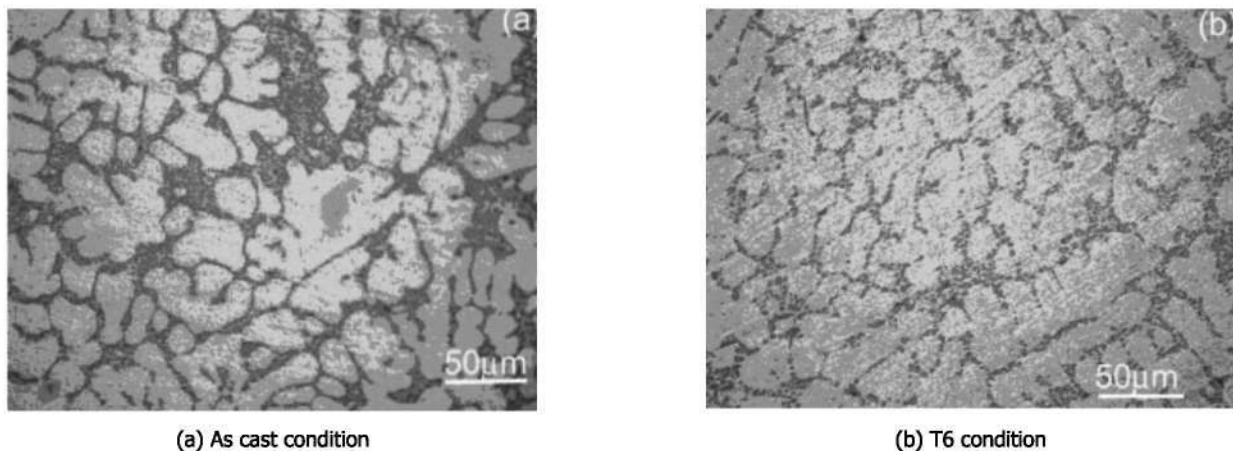Fig. 2 : Al-Si phase diagram showing the temperature range where PMZ formed.

(a) As cast condition

(b) T6 condition

Fig. 3 : Microphotographs of Base metal A356 alloy
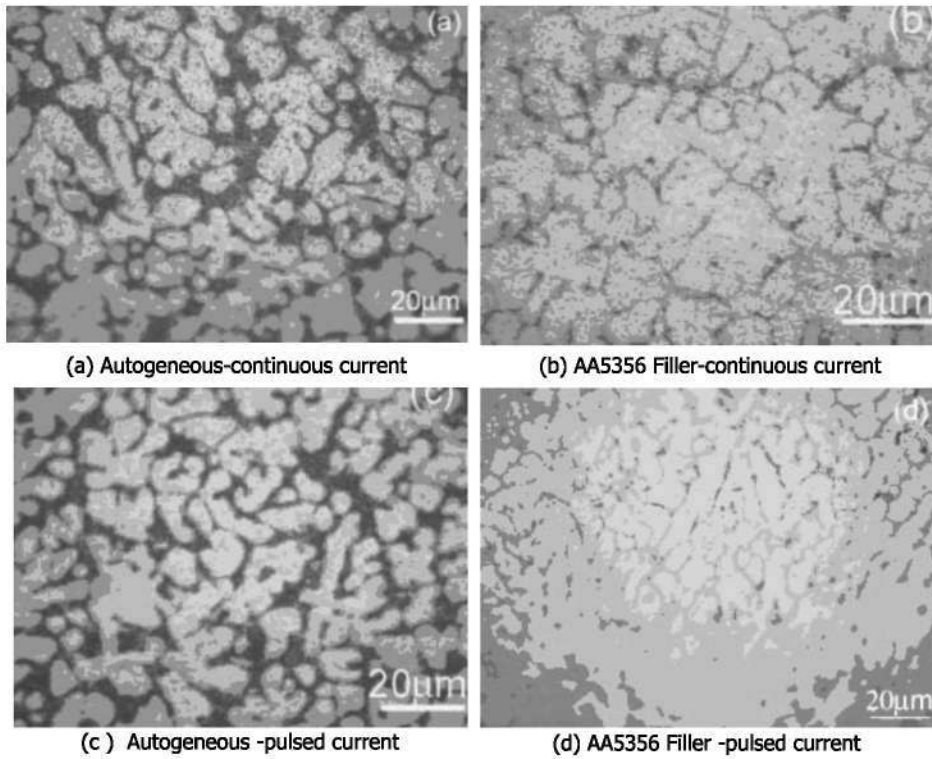
35

(a) Autogeneous-continuous current

(b) AA5356 Filler-continuous current

(c) Autogeneous -pulsed current

(d) AA5356 Filler -pulsed current

Fig.4 : Microphotographs of weld metal of GTAW A356 alloy in as cast condition

(a) Autogeneous -continuous current

(b) AA5356 Filler -continuous current

(c) Autogeneous - pulsed current

(d) AA5356 Filler -pulsed current
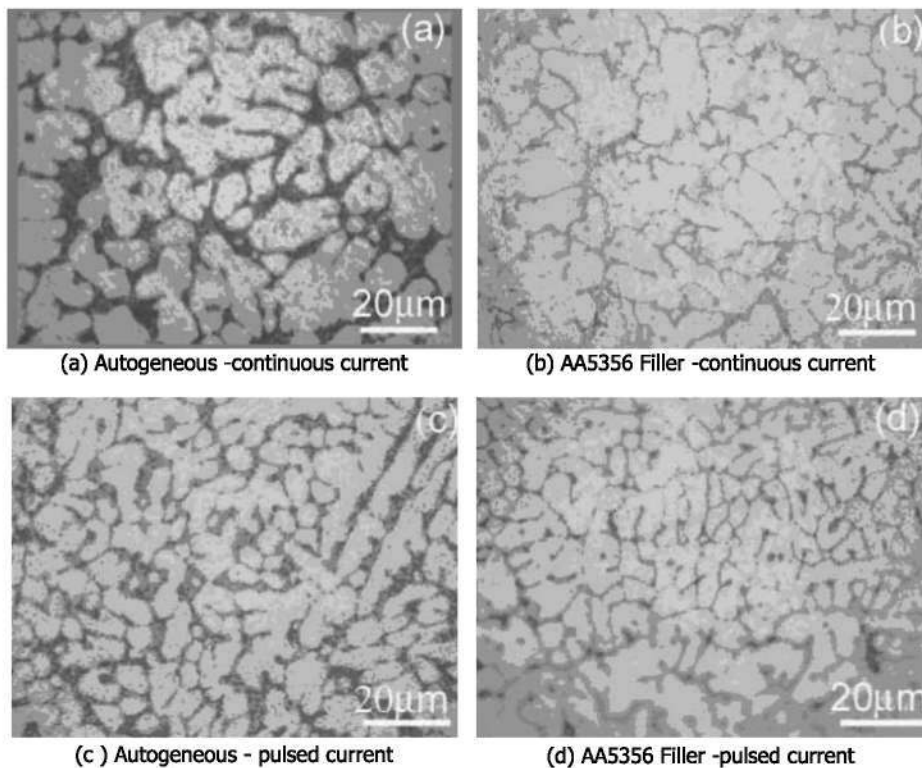
Fig. 5 : Microphotographs of weld metal of GTAW A356 alloy in T6 condition
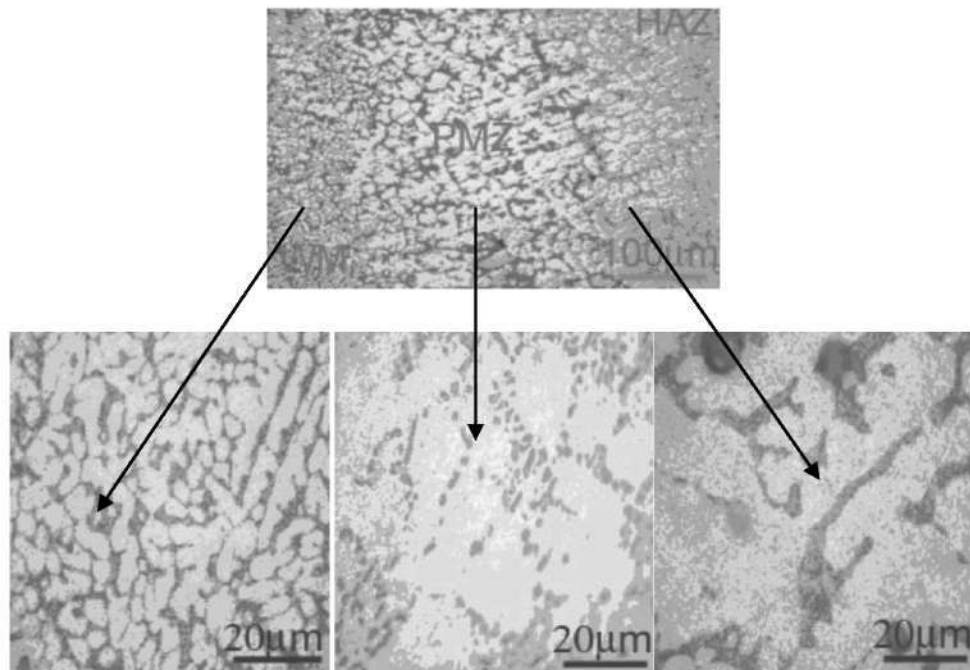
Fig.6 : Microphotographs of WM, PMZ and HAZ of PCGTAW T6- A356 alloy

(a) Autogeneous -continuous current

(b) AA5356 Filler -continuous current

(c) Autogeneous -pulsed current

(d) AA5356 Filler -pulsed current
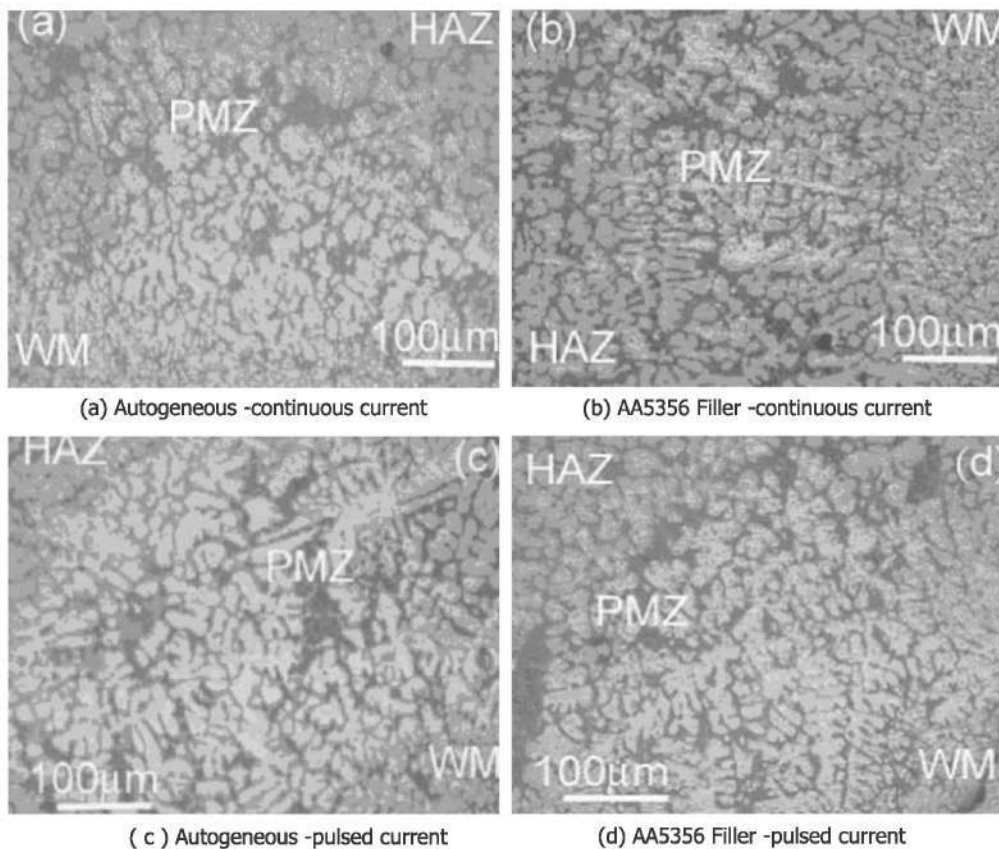
Fig. 7 : Microphotographs of weld metal, PMZ and HAZ of A356 alloy in as cast condition

(a) Autogeneous -continuous current

(b) AA5356 Filler -continuous current

(c) Autogeneous -pulsed current

(d) AA5356 Filler -pulsed current
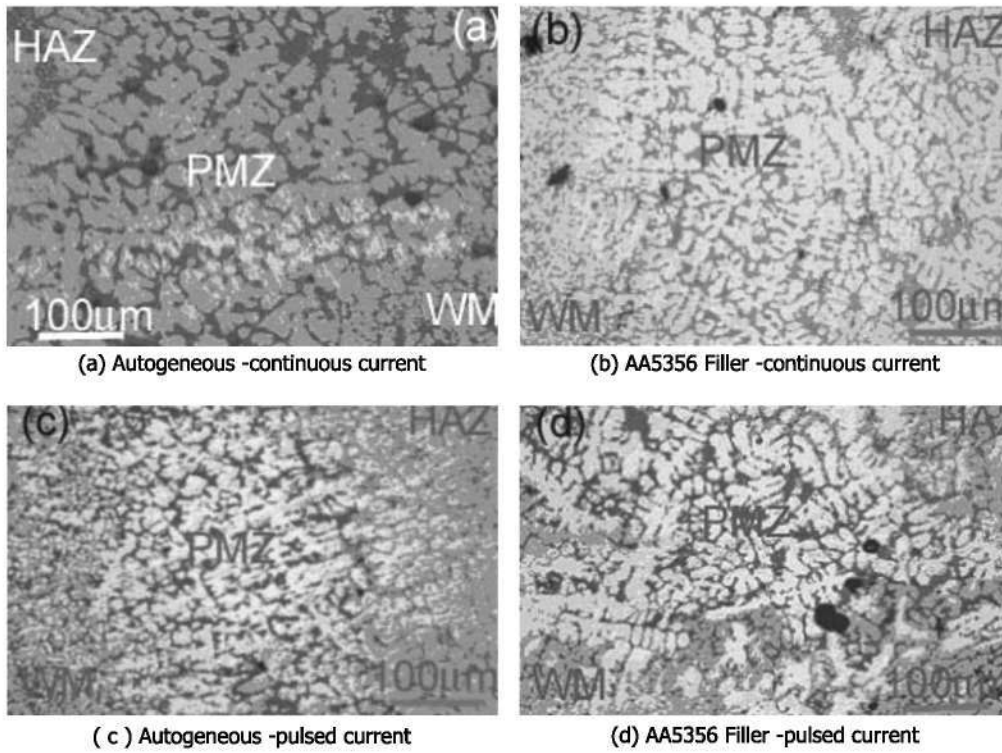
Fig.8 : Microphotographs of weld metal, PMZ and HAZ of A356 alloy in T6 condition

(a) Autogeneous -continuous current

(b) AA5356 Filler -continuous current

(c) Autogeneous -pulsed current

(d) AA5356 Filler -pulsed current

Fig. 9 : Microphotographs of pmz in GTAW A356 alloy in as cast condition

(a) Autogeneous -continuous current

(b) AA5356 Filler -continuous current

(c) Autogeneous -pulsed current

(d) AA5356 Filler -pulsed current
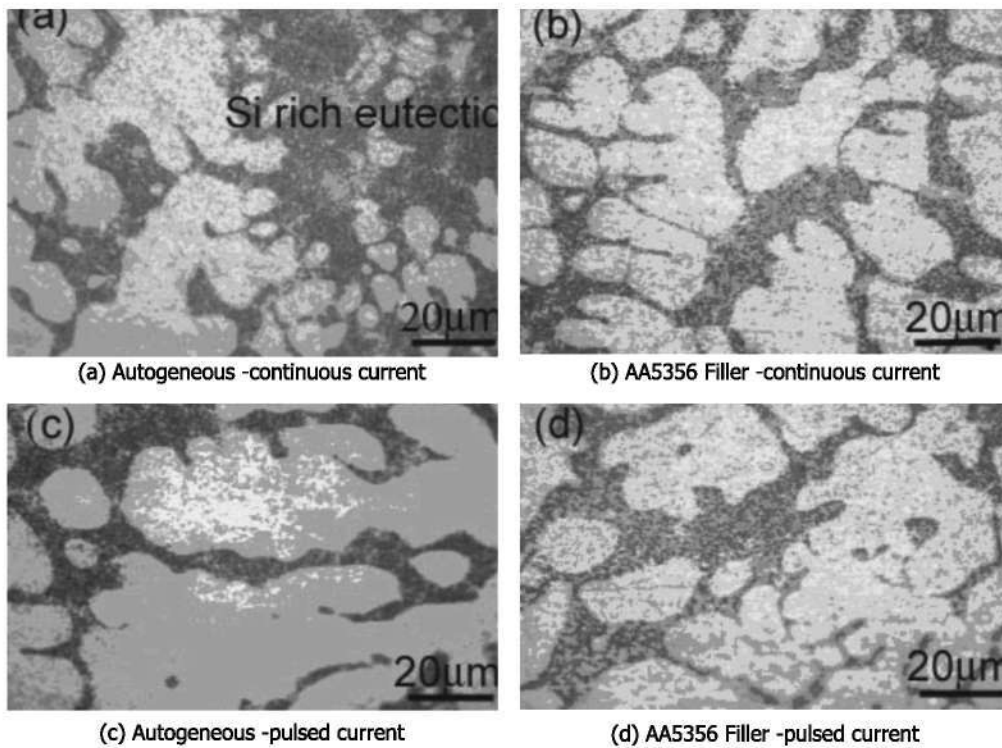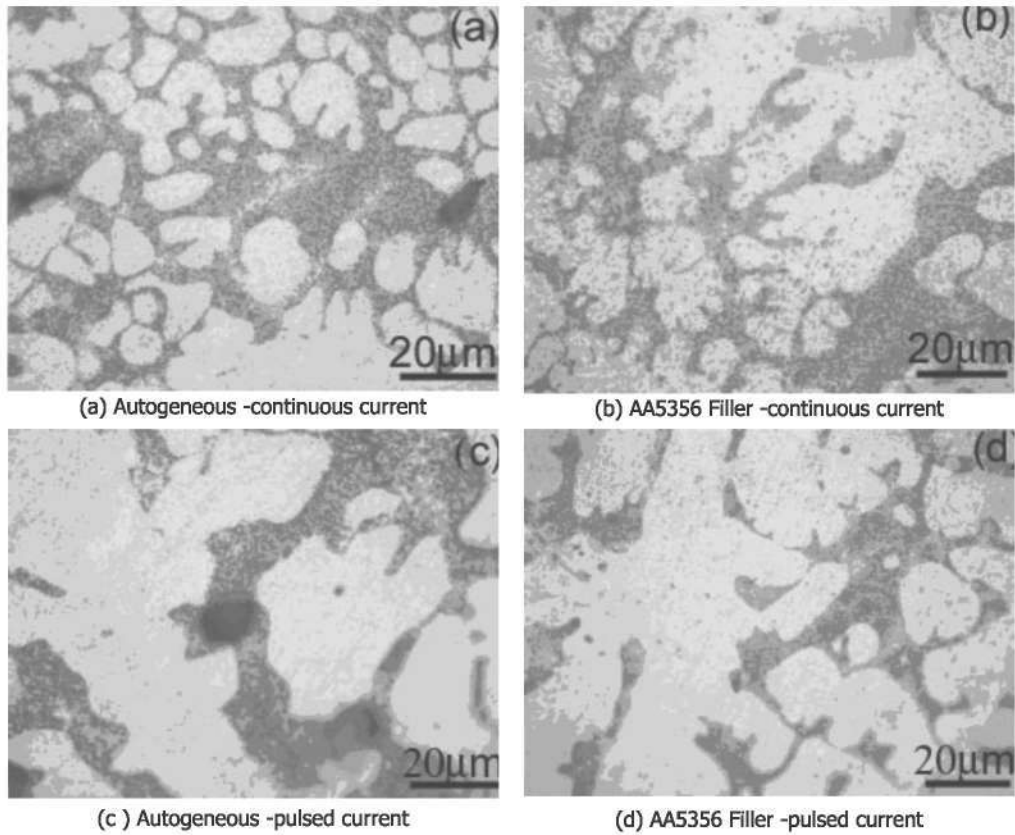
Fig. 10 : Microphotographs of pmz in GTAW A356 alloy in T6 condition
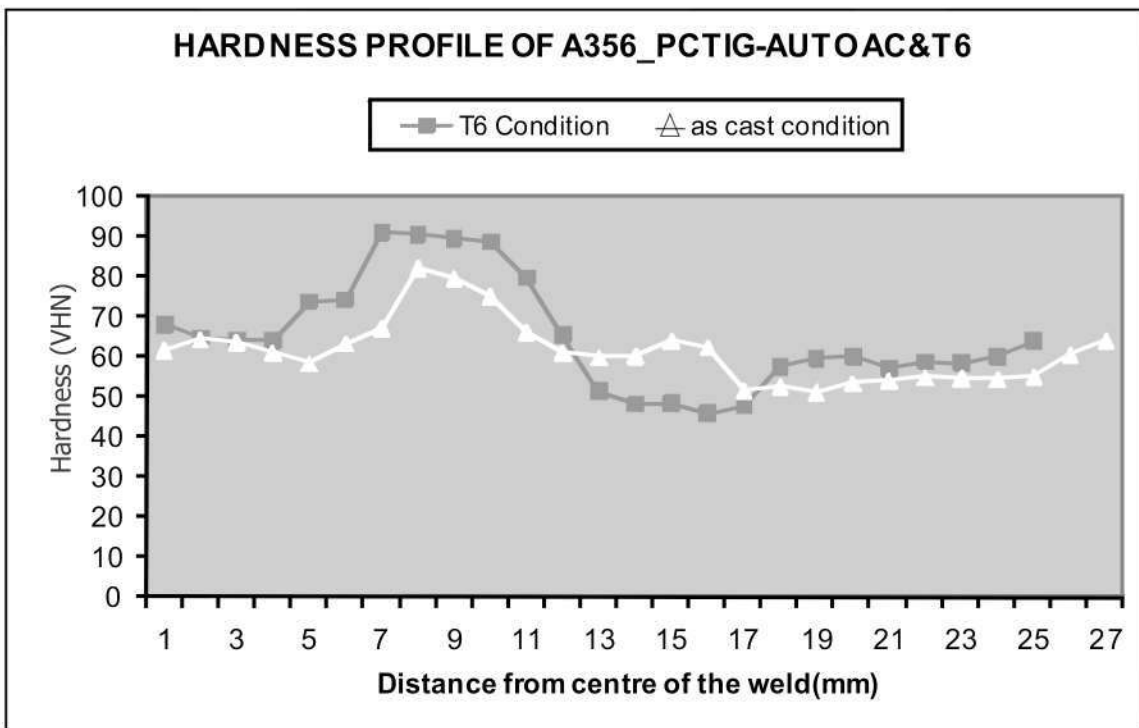
Fig. 11 : Comparison of Hardness profiles of autogenous GTAW A356 alloy in As cast and T6 conditions

HARDNESS PROFILE OF A356 -CCTIG-5356-AC & T6
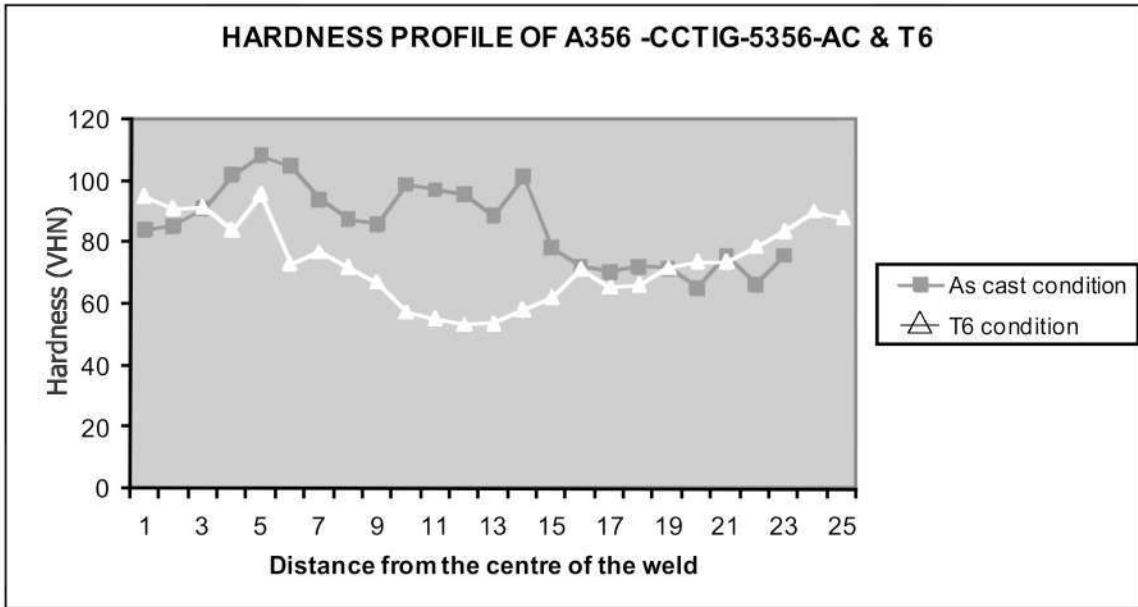
Fig. 12 : Comparison of Hardness profiles of GTAW (5356 filler) A356 alloy in As cast and T6 conditions
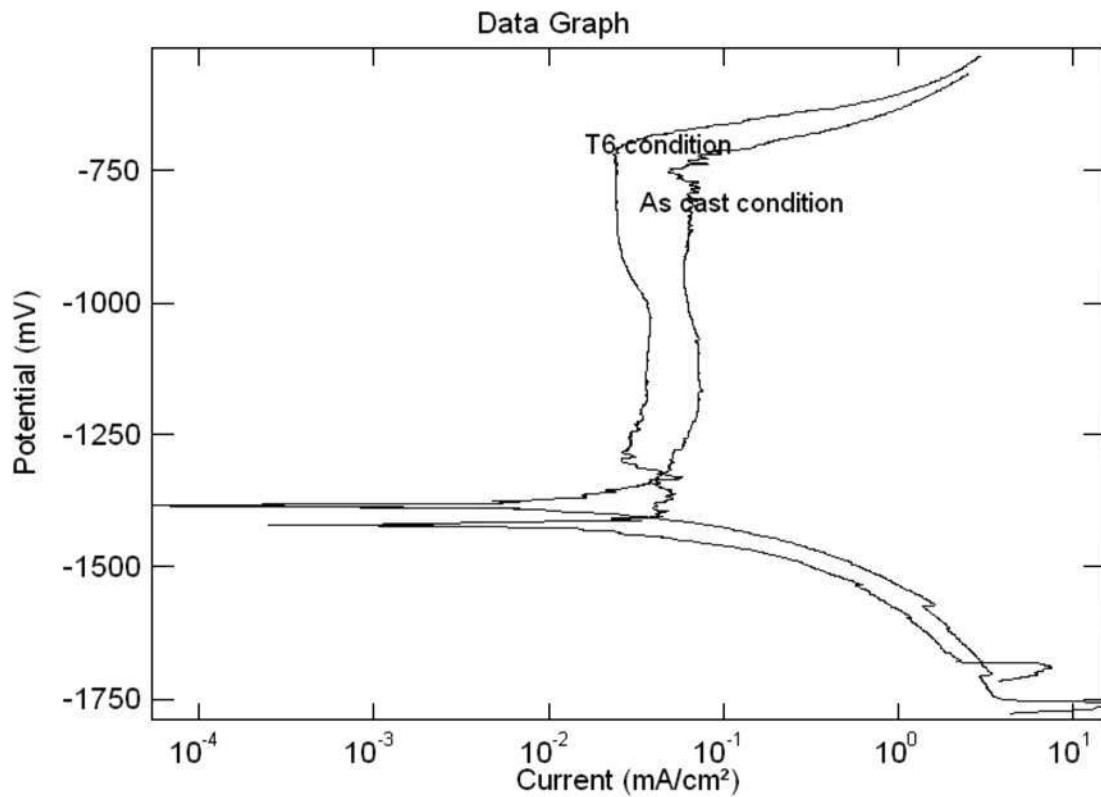
Fig. 13 : Potentiodynamic polarization curves of Base metal A356 alloy
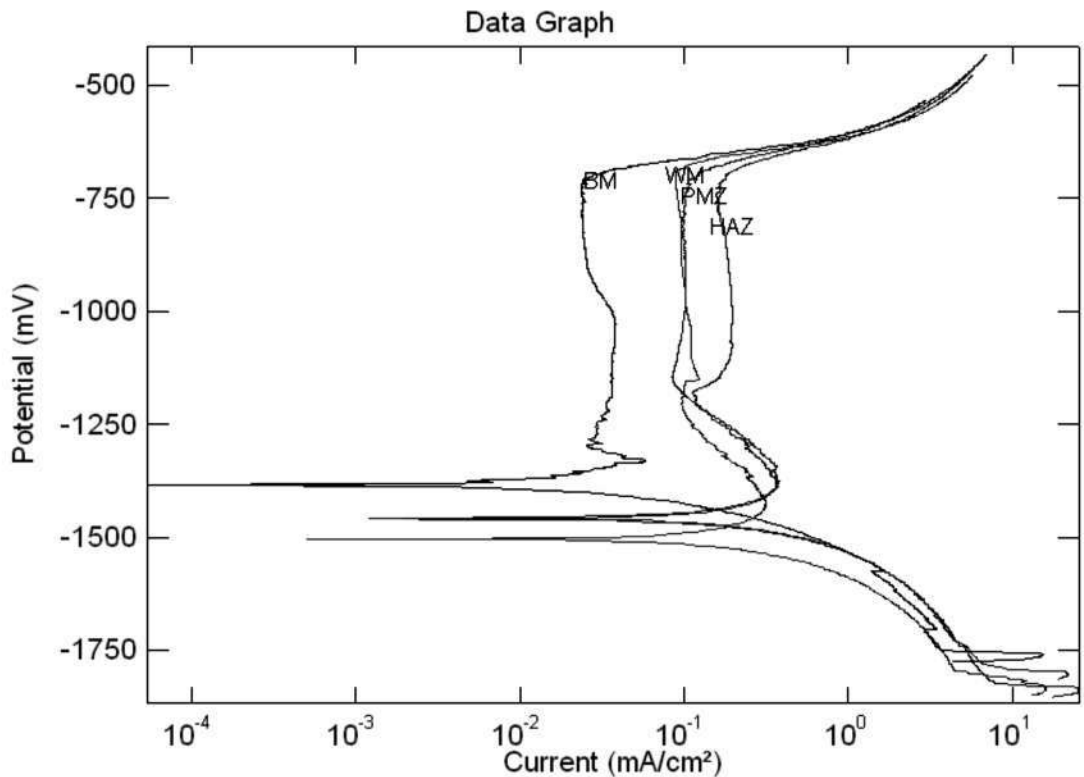
Fig. 14 : Potentiodynamic polarization curves of BM, WM, PMZ and HAZ in GTAW A356 alloy in T6 condition.
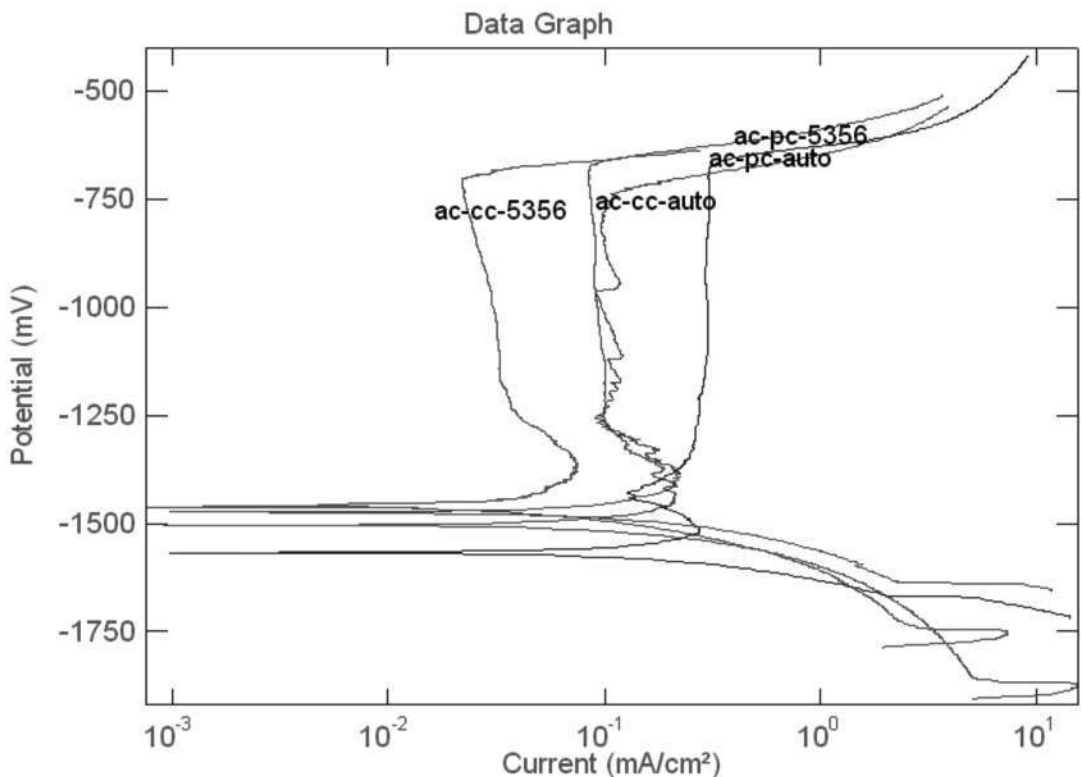

Fig. 15 : Potentiodynamic polarization curves of weld metal in GTAW A356 alloy in as cast condition
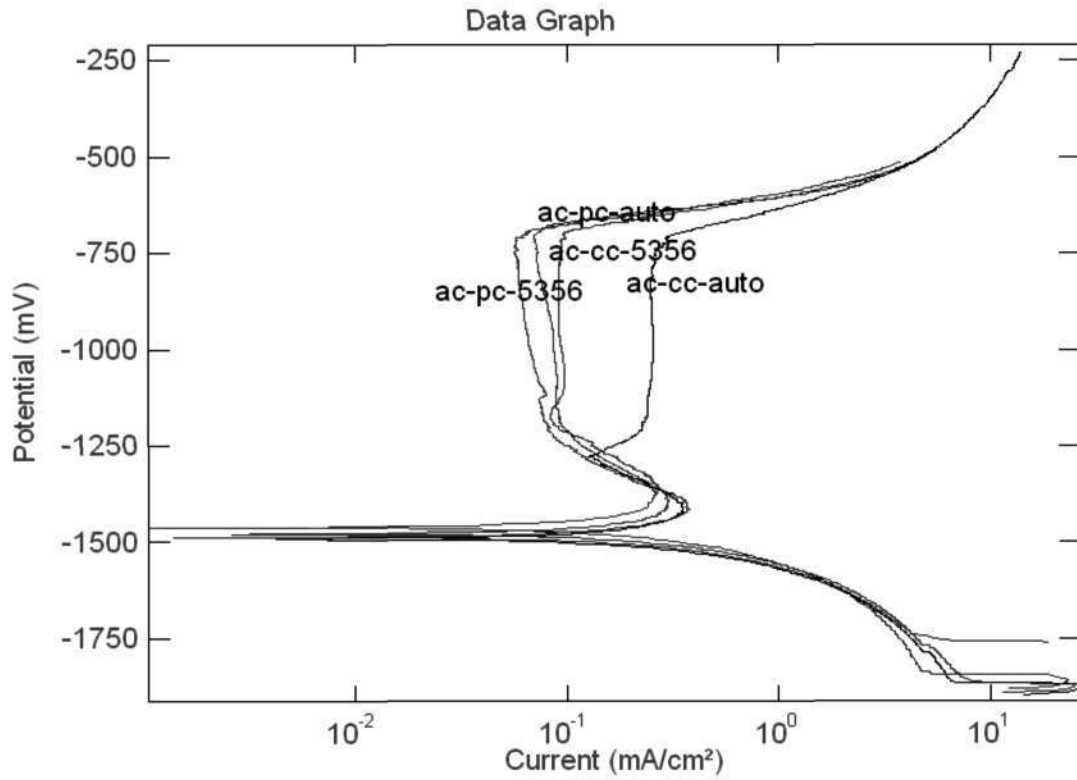
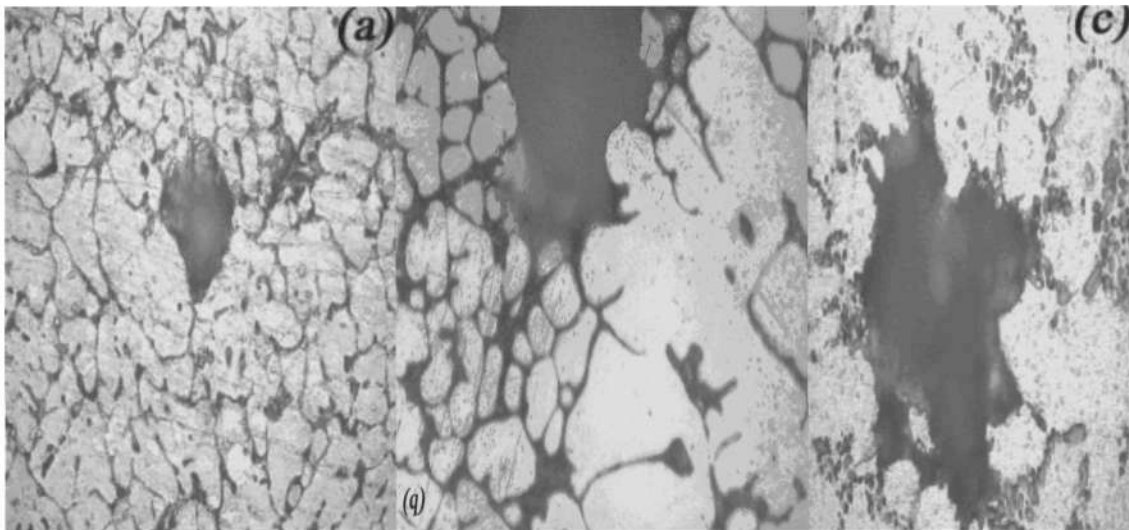Fig. 16 : Potentiodynamic polarization curves of PMZ in GTAW A356 alloy in as cast condition

Fig. 17 : Microphotographs of WM, PMZ and HAZ in PCGTAW A356 alloy in T6 condition